Available online at www.sciencedirect.com
SCIENCE DIRECT®
Journal of Nuclear Materials 349 (2006) 282–290
journal of nuclear materials
www.elsevier.com/locate/jnucmat

Deuterium retention in sintered boron carbide exposed to a deuterium plasma

V.Kh. Alimov [a], D.A. Komarov [a], J. Roth [b,*], M. Mayer [b], S. Lindig [b]

[a] Institute of Physical Chemistry, Russian Academy of Sciences, Leninsky Prospect 31, 117915 Moscow, Russia
[b] Max-Planck-Institut für Plasmaphysik, EURATOM Association, Boltzmannstrasse 2, D-85748 Garching, Germany

Received 26 August 2005; accepted 9 November 2005

Abstract

Depth profiles of deuterium up to a depth of 10 μm have been measured using the $D(^3He,p)^4He$ nuclear reaction in a resonance-like technique after exposure of sintered boron carbide, B_4C, at elevated temperatures to a low energy (≈200 eV/D) and high ion flux ($\approx 10^{21}$ m^{-2} s^{-1}) D plasma. The proton yield was measured as a function of incident ^3He energy and the D depth profile was obtained by deconvolution of the measured proton yields using the program SIMNRA. D atoms diffuse into the bulk at temperatures above 553 K, and accumulate up to a maximum concentration of about 0.2 at.%. At high fluences ($\geqslant 10^{24}$ D/m^2), the accumulation in the bulk plays a major role in the D retention. With increasing exposure temperature, the amount of D retained in B_4C increases and exceeds a value of 2×10^{21} D/m^2 at 923 K. The deuterium diffusivity in the sintered boron carbide is estimated to be $D = 2.6 \times 10^{-6} \exp\{-(107 \pm 10)\ \text{kJ mol}^{-1}/RT\}\ \text{m}^2\ \text{s}^{-1}$.

1. Introduction

Boron carbide is considered as a potential plasma facing material for fusion reactors due to its low atomic number, plasma compatibility, high melting point, and low chemical erosion yield [1]. A number of data on boron carbide for fusion applications have been reported concerning chemical erosion [2–9], physical sputtering [10–14], and retention of hydrogen isotopes [15–23]. Data on the transport properties of hydrogen isotopes in boron carbide structures were compiled by Grossman et al. [24].

The only solubility data for deuterium in boron carbide found in the literature are the TDS measurements of Shirasu et al. [25]. Those data closely obeyed Sievert's solubility law, indicating that hydrogen is in atomic form in the boron carbide. The enthalpy of solution was found to be -29.7 kJ mol^{-1}, and the negative sign indicates that hydrogen dissolves exothermally in boron carbide (i.e., the hydrogen solubility decreases with increasing temperature).

The saturation concentration of trapped deuterium is 0.4–0.6 D/(B + C) at room temperature [20,22]. There is some evidence that D atoms diffuse beyond the ion range both at room temperature, and at an elevated temperature of 403 K [22,18]. There are only very few data available about the temperature dependence of D retention in B_4C:

* Corresponding author. Tel.: +49 89 3299 1387; fax: +49 89 3299 2279.
E-mail address: roth@ipp.mpg.de (J. Roth).

0022-3115/$ - see front matter © 2005 Published by Elsevier B.V.
doi:10.1016/j.jnucmat.2005.11.002

These data were obtained by TDS measurements after irradiation with 1 keV D ions to a fluence of 2.3×10^{22} D/m^2 [18].

This work deals with deuterium retention in sintered B_4C exposed to a low energy (≈200 eV/D) and high ion flux (≈10^{21} m^{-2} s^{-1}) D plasma at elevated temperatures. Deuterium depth profiles were determined from the measurement of the proton yield as a function of incident ^{3}He energy and subsequent deconvolution of the obtained proton yield function.

2. Experimental

The samples with dimensions of $\sim 6 \times 6$ mm^2 and 1 mm thickness were made of sintered boron carbide B_4C (Tetrabor) with a density of 2.51 g/cm^3 supplied by Wacker-Chemie GmbH, Kempten, Germany. According to the specifications of the manufacturer, the bulk carbon concentration was 19–21 at.%.

The samples were exposed to a deuterium plasma at exposure temperatures T_{exp} between 553 K and 923 K. The plasma was generated in a planar dc magnetron, operated with D_2 gas at a pressure of about 1 Pa. The sample was attached to the magnetron cathode and covered with a copper mask. The D plasma exposure was done through an aperture of 5 mm in diameter.

The sample placed on the cathode surface was bombarded with plasma ions accelerated in the cathode sheath of the magnetron discharge with a discharge voltage of 450 V. For assessment of the ion energy, the spatial distribution of the plasma potential was measured using Langmuir probes [26]. The measurements showed that the cathode-drop voltage was about 0.85 of the discharge voltage. Reasoning that D_2^+ ions dominate in the plasma, the mean energy of D ions was estimated to be approximately 200 eV. The ion flux density was determined from ion current measurements and was around 1×10^{21} D/(m^2 s). All samples were exposed to the D plasma for 30 min, resulting in an ion fluence of about 2×10^{24} D/m^2. The sample temperature was controlled by a chromel–alumel thermocouple attached to the front surface of the sample outside the irradiation area during plasma exposure.

Deuterium depth profiles in the B_4C samples were determined by the $^3He + D \rightarrow p + \alpha$ nuclear reaction [27]. A ^{3}He beam was produced by the 3 MV tandem accelerator at IPP Garching. The D concentration within the near-surface layer (at depths up to 0.5 μm) was measured by means of the D(^{3}He,α)H reaction at a ^{3}He energy of 0.69 MeV. The α particles were energy-analyzed with a small-angle surface barrier detector at the laboratory scattering angle of 102°. The α spectrum was transformed into a D depth profile using the program SIMNRA [28].

To determine the D concentration at larger depths, an analyzing beam of ^{3}He ions with energies varied from 0.69 to 3.2 MeV was used. Protons emitted from the D(^{3}He,p)^{4}He nuclear reaction with

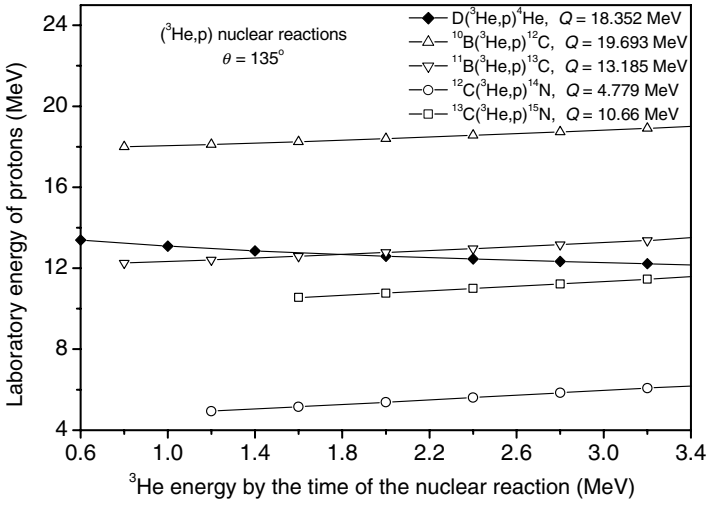

Fig. 1. Laboratory energy of protons from (^{3}He,p) nuclear reactions with D, ^{10}B, ^{11}B, ^{12}C and ^{13}C atoms at a laboratory angle of 135° as a function of ^{3}He energy. Q is the energy released in the nuclear reaction [29,30].

energies in the range 12.2–13.3 MeV (depending on ^{3}He energy, Fig. 1) were detected using a wide-angle surface barrier detector with a solid angle of 0.14 sr and a depletion depth of 700 μm, located at a laboratory angle $\theta = 135°$. A Ni absorber foil with a thickness of 20 μm and a 150 μm stainless steel foil were positioned in front of the detector. These foils absorb elastically scattered ^{3}He ions, α particles from the D(^{3}He,α)H nuclear reaction, and protons from the ^{12}C(^{3}He,p$_{0,1,2}$)^{14}N reactions. High energetic protons from the D(^{3}He,p)^{4}He, ^{10}B(^{3}He,p$_{0,1}$)^{12}C, ^{11}B(^{3}He,p$_{0,1,2,3}$)^{13}C and ^{13}C(^{3}He,p$_{0,1,2}$)^{15}N reactions (Fig. 1) can reach the detector. After loosing energy in the foils, these protons are fully stopped in the detector (except the 18–19 MeV protons from the ^{10}B(^{3}He, p$_0$)^{12}C reaction, which loose only a fraction of their energy in the detector). The proton energies for the ^{3}He + ^{11}B and ^{3}He + ^{13}C nuclear reactions partially overlap with protons from the ^{3}He + D nuclear reaction (Fig. 1). The proton yield from the ^{3}He + (^{10}B/^{11}B/^{13}C) nuclear reactions was determined in separate measurements using original B_4C samples without implanted D atoms. The yields obtained from these reactions were then subtracted from the measured total proton yield for the plasma exposed B_4C (Fig. 2).

In order to determine the D concentration profile in deeper layers, the computer program SIMNRA [28] was used for the deconvolution of the proton yields measured at different ^{3}He ion energies. A deuterium depth distribution was assumed, taking into account the near-surface depth profile obtained from the α particles spectrum, and the proton yield was calculated as a function of incident ^{3}He energy. The form of the D depth profile was then varied using an iterative technique until the calculated curve matched the measured proton yields [27].

To understand in which state deuterium was retained in the sintered B_4C, sputtering secondary ion mass spectrometry (SIMS) and residual gas analysis (RGA) were utilized for analysis of the plasma-exposed samples. We attribute the appearance of the SIMS D^- signal to the existence of separate D atoms within the matrix [31]. A reason for appearance of the RGA D_2 signal is the recombination of D atoms, as well as the direct release of

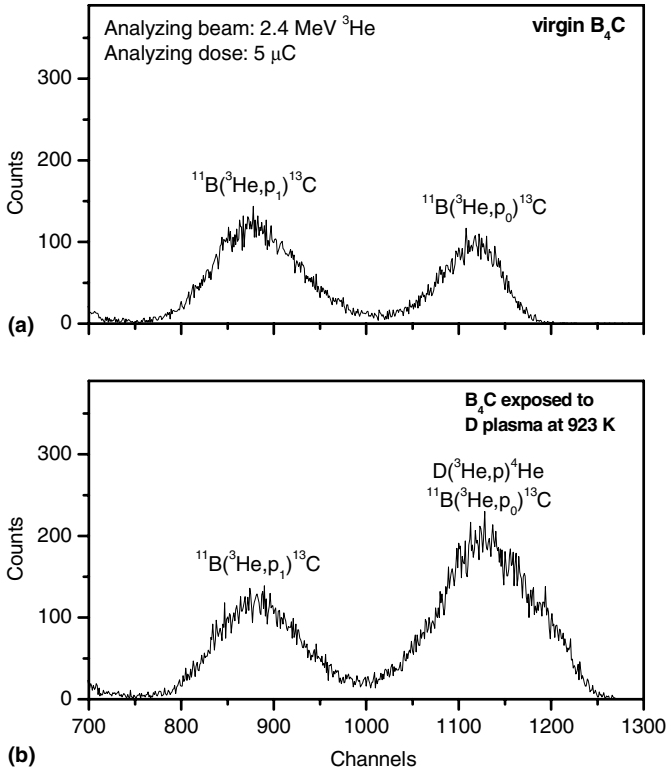

Fig. 2. Proton spectra obtained by 2.4 MeV ^{3}He bombardment of the B_4C. (a) unexposed B_4C. (b) exposed to a low-energy (≈200 eV/D) deuterium plasma to a fluence of about 2×10^{24} D/m^2 at 923 K.

D_2 molecules from the sputtered layers. The procedure, how to separate the recombined and molecular fractions has been described in Ref. [31]. The D^- SIMS signal was calibrated by using sintered B_4C implanted with 3 keV D ions at 300 K to fluences below 1×10^{21} D/m^2 (when 100% trapping takes place) by comparing the integrated SIMS signal (throughout the implantation depth) with the total amount of deuterium in this sample. The error of the calibration was estimated to be about 30%.

3. Results and discussion

Both, after 3 keV D ion irradiation at 300 K and after D plasma exposure at temperatures in the range from 553 to 923 K, D_2 molecules were not detected in the RGA measurements. It is therefore concluded that deuterium is accumulated in the sintered B_4C solely as D atoms.

Measured proton yields as a function of the analyzing ^{3}He energy for the boron carbide exposed to the low energy (≈200 eV/D) and high ion flux (≈10^{21} m^{-2} s^{-1}) D plasma to a fluence of about 2×10^{24} D/m^2 at different temperatures T_{exp} are shown in Fig. 3. The corresponding D depth profiles are presented in Fig. 4, where the upper part shows the depth profiles in the near-surface layer (at depths up to 0.5 μm) and the lower part shows the profiles in the bulk (up to 10 μm).

As the exposure temperature T_{exp} increases, the D concentration in the near surface layers decreases (Fig. 4a), whereas the concentration in the bulk increases (Fig. 4b). At $T_{exp} = 923$ K, the D profile has a long tail extending beyond 10 μm with a D concentration of about 0.2 at.%.

SEM micrographs of the B_4C samples before and after plasma exposure are shown in Fig. 5. After plasma exposure, 'pin holes' extending at least up to a depth of 1 μm are observed on the surface. It is possible that the development of these holes is connected with the formation and emission of CD_4 molecules in the course of the D plasma exposure [5–7,18].

Fig. 6 compares the deuterium retention in the boron carbide samples exposed to the D plasma to a fluence of about 2×10^{24} D/m^2 (high fluence exposure), with previous results on 1 keV D ion irradiation to fluences of $(2.3–2.7) \times 10^{22}$ D/m^2 (low fluence irradiation) [18,22] as a function of the exposure/irradiation temperature. Note that the D content in the B_4C irradiated with 1 keV D ions to the low fluences was measured by thermal desorption spectroscopy, whereas the D content after plasma exposure to the high fluence was determined by depth profiling up to a depth of 10 μm.

At low fluence irradiation the D retention is governed by the accumulation of D in the ion implanted zone and the fraction of D atoms which diffused

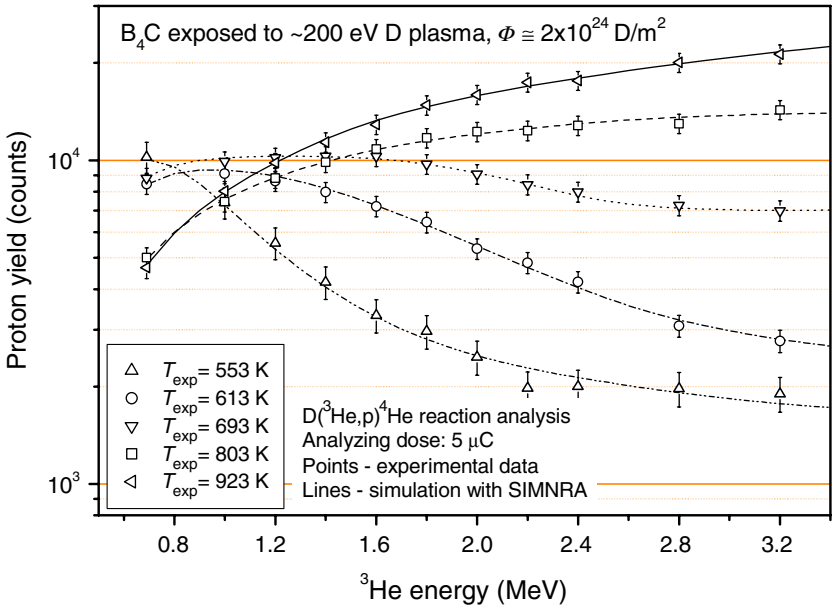

Fig. 3. Measured (points) and calculated (lines) proton yields for assumed D profiles (see Fig. 4) as a function of the analyzing ^{3}He energy for B_4C exposed to a low-energy (≈200 eV/D) deuterium plasma to a fluence of about 2×10^{24} D/m^2 at different temperatures.

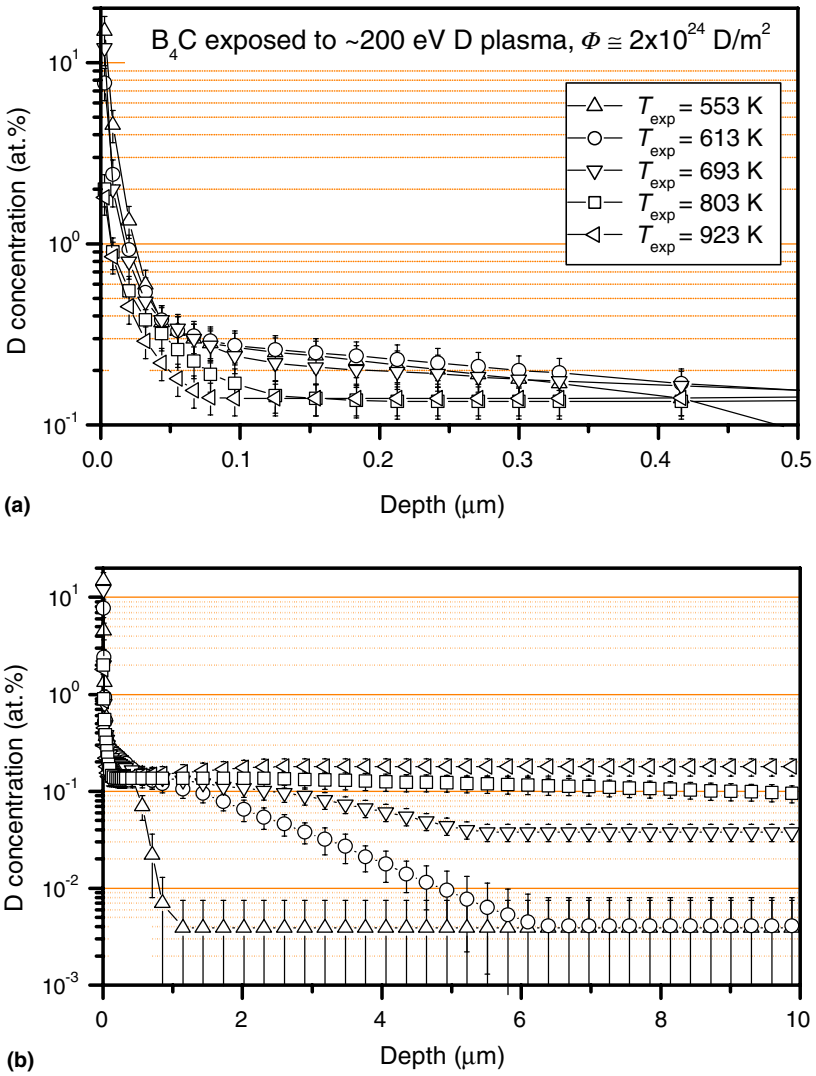

Fig. 4. Depth profiles of deuterium trapped in the near-surface layer (a) and in the bulk (b) of B_4C exposed to a low-energy (≈200 eV/D) deuterium plasma to a fluence of about 2×10^{24} D/m^2 at different temperatures. The D concentration up to 0.5 μm (a) was determined from the energy spectra of α particles emitted from the D(^{3}He,α)H reaction. Note that the depth and concentration scales in parts (a) and (b) are different.

into the bulk is small compared to high fluence exposure. As the irradiation/exposure temperature increases, the D concentration in the ion implanted zone decreases resulting in a decrease of the total D content with increasing temperature (Fig. 6, data for the 1 keV D ion irradiation). At high fluences, however, the amount of deuterium accumulated in the bulk increases with irradiation temperature as the implanted D atoms begin to diffuse into the bulk, where they are retained at trapping sites, probably at carbon precipitates. Because the amount of deuterium accumulated in the bulk is higher than in the implanted zone, an increase of the total D content with exposure temperature is observed (Fig. 6, data for the plasma exposure).

The analysis of the D profiles in the B_4C samples allows the conclusion that there are two channels for deuterium diffusion. A 'fast' diffusion channel enables the penetration of D atoms deep into the bulk (up to 10 μm) even at $T_{exp} = 553$ K, and the formation of flat D profile with concentrations of about 4×10^{-3} at.% at 553 K and about 4×10^{-2} at.% at 693 K (Fig. 4b). A 'slow' diffusion channel is responsible for the gradient of the deuterium profiles from a maximum concentration of 0.1–0.2 at.% to the bulk values.

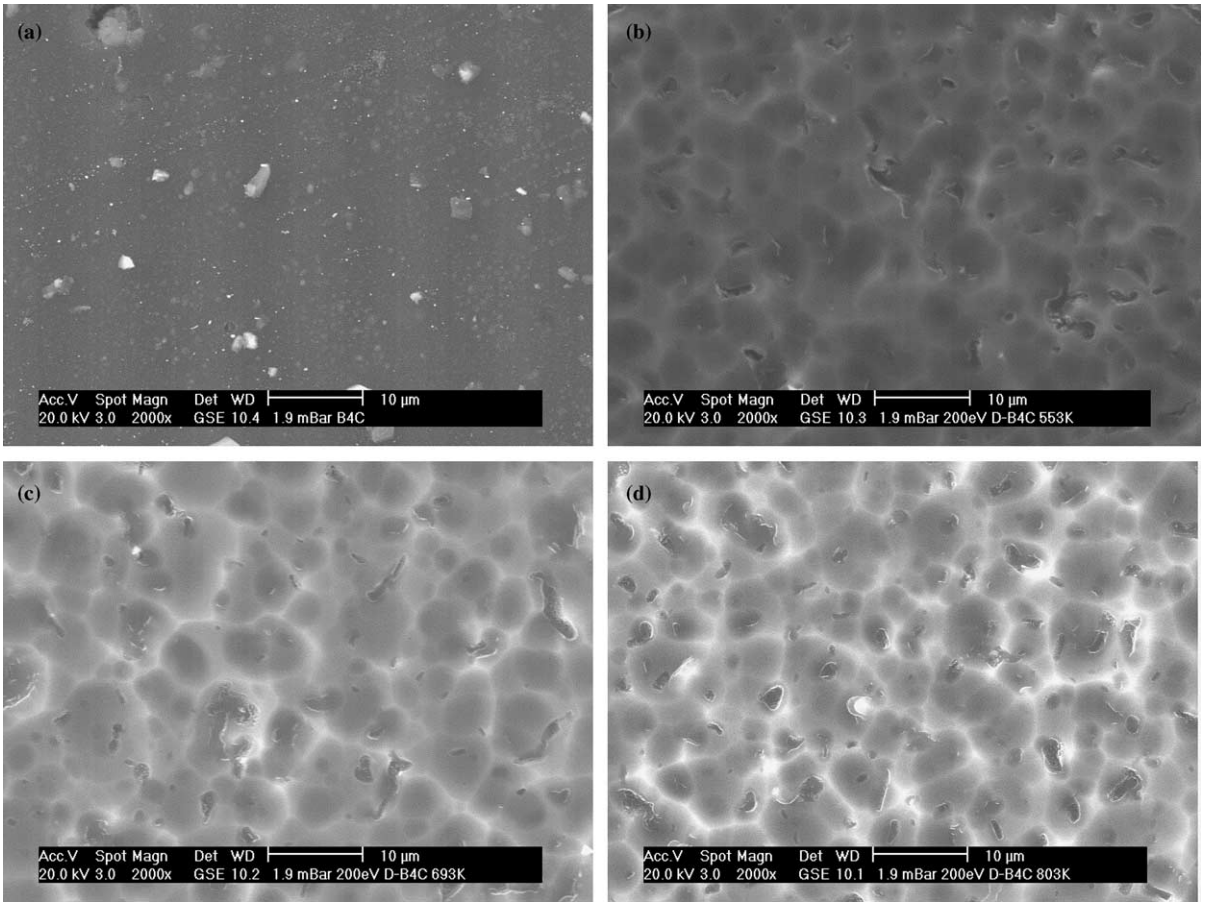

Fig. 5. SEM micrographs of the sintered boron carbide B_4C before (a) and after D plasma exposure to a fluence of about 2×10^{24} D/m^2 at exposure temperatures of 553 K (b), 693 K (c) and 803 K (d).

Based on the measured depth profiles, it is possible to estimate the D diffusivity in the 'slow' channel, assuming that the deuterium profile is governed by diffused D atoms. If a constant deuterium concentration C_0 is maintained at the surface (or in a thin near-surface layer), the D concentration $C(x)$ at a depth x is described by

$$C(x) = C_0\left[1 - \mathrm{erf}\left(\frac{x}{2\sqrt{Dt}}\right)\right], \quad (1)$$

where $\mathrm{erf}\left(\frac{x}{2\sqrt{Dt}}\right)$ is the error function, D is the deuterium diffusivity and t is the exposure time [32]. The concentration C_0 and the deuterium diffusivity are varied until the calculated profile matches the measured D profile (Fig. 7 and Table 1). According to our estimation, the diffusivity of deuterium in the sintered boron carbide through the 'slow channel' is $D = 2.6 \times 10^{-6}\exp\{-E_A/RT\}$ m^2 s^{-1} with an activation energy $E_A = (107 \pm 10)$ kJ mol^{-1}.

Fig. 8 shows a comparison of the estimated deuterium diffusivity with other available results on tritium diffusivity [33–38], derived from the thermal release data treating the grain structure as 'diffusion out of a sphere'. Elemann et al. [33–35] used boron carbide samples that were doped with tritium in a surface layer of about 20 μm thickness. The tritons were produced via the reaction ^{6}Li(n,α)T induced by thermal neutrons. The neutron dose was 2×10^{18} n/m^2, such that the determined activation energy of (70 ± 7) kJ mol^{-1} is characteristic for tritium mobility in a low-dose irradiated material. The same is true for the results obtained by Schnarr and Münzel [37]. They used samples which were uniformly doped with high energy (<90 MeV) tritons produced in the reaction Cu(α,T), induced by 104 MeV α-particles. The effective diffusion coefficients with an activation energy of (95 ± 10) kJ mol^{-1} are about one order of magnitude higher than the values obtained by Elleman et al. [33–35].

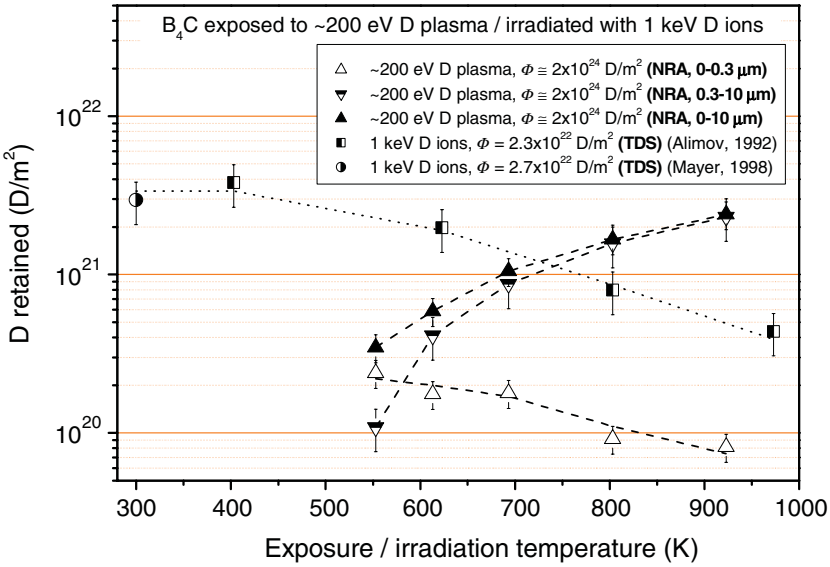

Fig. 6. Amount of deuterium trapped in B_4C (i) exposed to a low-energy (≈200 eV/D) deuterium plasma to a fluence of about 2×10^{24} D/m^2, and (ii) irradiated with 1 keV D ions to fluences of 2.3×10^{22} D/m^2 [18] and 2.7×10^{22} D/m^2 [22] as a function of the exposure/irradiation temperature. For B_4C exposed to the D plasma, the D retention in the near-surface layers (at depths from 0 to 0.3 μm) and in the bulk (at depths from 0.3 to 10 μm) is shown additionally.

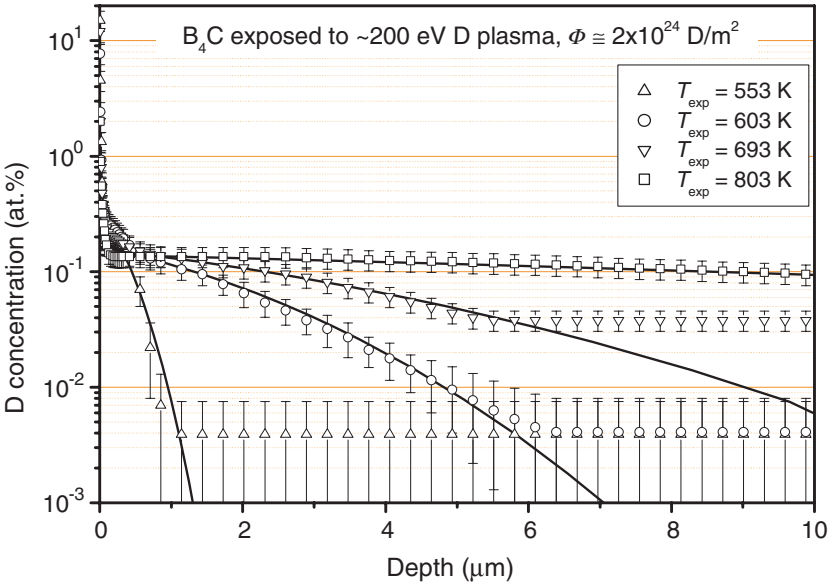

Fig. 7. Measured (symbols) and calculated (lines) deuterium depth profiles in B_4C exposed to a low-energy (≈200 eV/D) deuterium plasma to a fluence of about 2×10^{24} D/m^2 at different temperatures.

This deviation might be due to the value of the grain radii used in the calculation.

Note that under neutron irradiation tritium is formed in boron carbide via the reaction $^{10}B(n,2\alpha)T$. Using boron carbide samples irradiated with low and high doses of neutrons, Schnarr and Münzel [36] found that the effective diffusion coefficient decreases by three orders of magnitude with increasing neutron dose, and attributed this decrease in tritium mobility to the radiation defects formed in the boron carbide. For the low dose of about 10^{20} n/m^2 of 22 MeV neutrons an activation

Table 1
Diffusion coefficient of deuterium in sintered boron carbide derived by fitting calculated diffusion profiles (Eq. (1)) to the measured deuterium depth profiles (Fig. 7)

Exposure temperature (K)	C_0 (at.%)	Diffusion coefficient (m^2/s)
553	0.32	1.09×10^{-16}
613	0.165	3.67×10^{-15}
693	0.157	1.32×10^{-14}
803	0.14	3.09×10^{-13}

energy of (87 ± 10) kJ mol^{-1} was found. At a high neutron dose of 3.5×10^{22} n/m^2 from a heavy water reactor, they found an activation energy of (210 ± 30) kJ mol^{-1} in the irradiated material, which was much higher than in the low-dose irradiated material. Suhaimi et al. [38] used the boron carbide samples exposed to neutrons with an average energy of 6.5 MeV and a dose of 10^{18} n/m^2, which is a low radiation dose. The reported activation energy is (196 ± 30) kJ mol^{-1}, which is high and more typical of radiation damaged material. The present data with an activation energy of (107 ± 10) kJ mol^{-1} are indicative for diffusion in an undamaged matrix. This may be the reason why the diffusion coefficients derived from the deuterium depth profiles are about one order of magnitude higher than the diffusion coefficients of tritium in B_4C samples irradiated with low doses of neutrons (Fig. 8).

The 'fast' deuterium diffusivity is assumed to be related to the movement of deuterium atoms along grain boundaries, whereas the 'slow' diffusion channel may be explained by intra-grain diffusion. The boron carbide structure may be implied to consist of single large continuous grains riddled with grain boundaries. The density of deuterium trap sites (most likely, carbon impurities) within the grains is thought to be significantly higher than that along the grain boundaries, such that the maximum deuterium concentration reached through the 'slow' diffusion channel (0.1–0.2 at.%, depending on the exposure temperature) is much higher than that for the 'fast' diffusion channel (about 4×10^{-3} at.% at 553–613 K and about 4×10^{-2} at.% at 693 K).

4. Conclusions

The retention of deuterium was studied in sintered boron carbide samples exposed to a low energy (≈200 eV/D) and high ion flux (≈10^{21} m^{-2} s^{-1}) D plasma at elevated temperatures. Trapping of deuterium molecules is not observed, and deuterium is accumulated as D atoms only.

At temperatures above 553 K, D atoms diffuse into the bulk and accumulate up to a maximum concentration of about 0.2 at.%. At high fluences ($\geqslant 10^{24}$ D/m^2), the accumulation in the bulk plays the major role for the D retention. With increasing

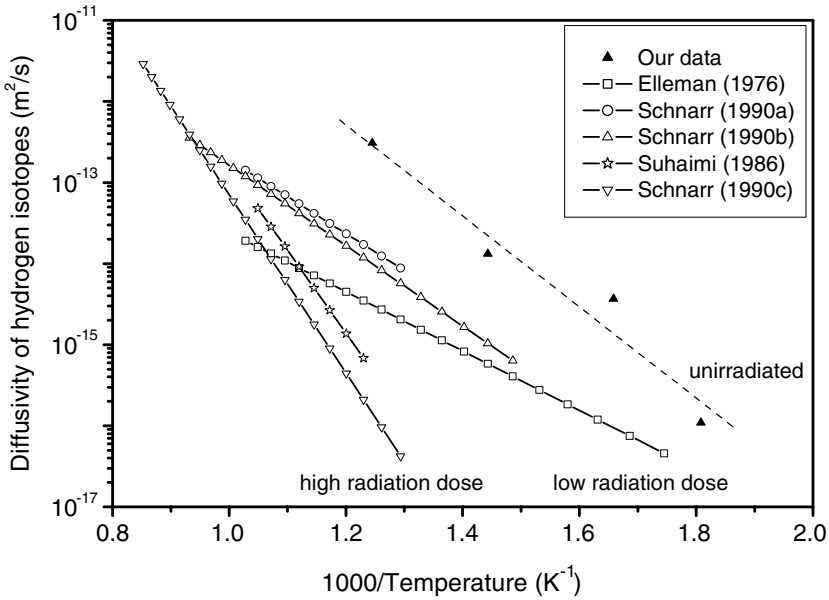

Fig. 8. Comparison of the Arrhenius relations for diffusivities of deuterium and tritium in boron carbides. The tritium diffusivity data were taken from Elleman et al. [33–35], Schnarr and Münzel ((a) [36], (b) [37], (c) [36]), and Suhaimi et al. [38].

exposure temperature, the amount of D retained in B_4C increases and exceeds a value of 2×10^{21} D/m^2 at 923 K.

There are two channels for deuterium diffusion. A 'fast' diffusion channel allowing the penetration of D atoms deep into the bulk (at least up to a depth of 10 μm) even at $T_{exp} = 553$ K, and resulting in the formation of the flat-shaped D profile with concentrations of about 4×10^{-3} at.% at 553–613 K and about 4×10^{-2} at.% at 693 K. A 'slow' diffusion channel provides the gradient of the deuterium profiles from a maximum concentration of 0.1–0.2 at.% into the bulk. In the 'slow' channel the deuterium diffusivity is estimated to be $D = 2.6 \times 10^{-6} \exp\{-(107 \pm 10\ \text{kJ mol}^{-1})/RT\}\ \text{m}^2\ \text{s}^{-1}$.

Acknowledgements

We express our appreciation to J. Dorner and M. Fußeder for their technical assistance with the ^{3}He beam analyses. One of us, V. Alimov, gratefully acknowledges financial support from the Max-Planck-Institut für Plasmaphysik and is candidly indebted to his colleagues from the Bereich Materialforschung of the IPP for their warm hospitality during his stay in Garching. The portion of this work performed at the Institute of Physical Chemistry, Moscow, was supported by the US Department of Energy under Contract No. LG-9196 with Sandia National Laboratories.

References

[1] O.I. Buzhinskij, Yu.M. Semenets, Fusion Eng. Des. 45 (1999) 343.
[2] S. Vepřek, M.R. Haque, H.R. Oswald, J. Nucl. Mater. 63 (1976) 405.
[3] C. Braganza, G. McCracken, S.K. Erents, in: Proceedings of the International Symposium on Plasma–Wall Interaction, Pergamon, 1977, p. 257.
[4] G.M. McCracken, P.E. Stott, Nucl. Fusion 19 (1979) 886.
[5] J.W. Davis, A.A. Haasz, J. Nucl. Mater. 175 (1990) 117.
[6] C. García-Rosales, E. Gauthier, J. Roth, R. Schwörer, W. Eckstein, J. Nucl. Mater. 189 (1992) 1.
[7] Y. Gotoh, T. Yamaki, T. Ando, R. Jimbou, N. Ogiwara, M. Saidoh, K. Teruyama, J. Nucl. Mater. 196–198 (1992) 708.
[8] B.M.U. Scherzer, V.Kh. Alimov, J. Nucl. Mater. 196–198 (1992) 703.
[9] T. Yamaki, Y. Gotoh, T. Ando, K. Teruyama, J. Nucl. Mater. 220–222 (1995) 771.
[10] J. Bohdansky, H.L. Bay, W. Ottenberger, J. Nucl. Mater. 76&77 (1978) 163.
[11] J. Roth, J. Bohdansky, A.P. Martinelli, Radiat. Effects 48 (1980) 213.
[12] J. Bohdansky, J. Roth, J. Nucl. Mater. 122&123 (1984) 1417.
[13] J.N. Brooks, J. Nucl. Mater. 93&94 (1980) 437.
[14] E. Hechtl, A. Mazanec, W. Eckstein, J. Roth, C. García-Rosales, J. Nucl. Mater. 196–198 (1992) 713.
[15] T.E. Boothe, H.J. Ache, J. Nucl. Mater. 84 (1979) 85.
[16] B.L. Doyle, W.R. Wampler, D.K. Brice, S.T. Picraux, J. Nucl. Mater. 93&94 (1980) 551.
[17] T. Maruyama, T. Iseki, J. Nucl. Mater. 133&134 (1985) 727.
[18] V.Kh. Alimov, R. Schwörer, B.M.U. Scherzer, J. Roth, J. Nucl. Mater. 187 (1992) 191.
[19] V. Fernandez, J. Bardon, E. Gauthier, C. Grisolia, J. Nucl. Mater. 196–198 (1992) 1022.
[20] R. Jimbou, M. Saidoh, N. Ogiwara, T. Ando, K. Morita, Y. Muto, J. Nucl. Mater. 196–198 (1992) 958.
[21] R. Jimbou, N. Ogiwara, M. Saidoh, K. Morita, K. Mori, B. Tsuchiya, J. Nucl. Mater. 220–222 (1995) 869.
[22] M. Mayer, M. Balden, R. Behrisch, J. Nucl. Mater. 252 (1998) 55.
[23] Y. Yamauchi, Y. Hirohata, T. Hino, K. Masaki, M. Saidoh, T. Ando, D.G. Whyte, C. Wong, J. Nucl. Mater. 266–269 (1999) 1257.
[24] A.A. Grossman, R.P. Doerner, S. Luckhardt, R. Seraydarian, A.K. Burnham, J. Nucl. Mater. 266–269 (1999) 819.
[25] Y. Shirasu, S. Yamanaka, M. Miyake, J. Alloys Compd. 190 (1992) 87.
[26] V.V. Zaitzev, A.E. Obruchnikov, D.A. Komarov, Measurements of temperature and density of electrons in dc magnetron plasma, in: Proceedings of the 4th International Symposium on Diamond Films and Related Materials, Kharkov, Ukraine, September 20–22, 1999, p. 331 (in Russian).
[27] V.Kh. Alimov, M. Mayer, J. Roth, Nucl. Instrum. and Meth. 234 (2005) 169.
[28] M. Mayer, SIMNRA User's Guide, Tech. Rep. IPP 9/113, Garching, 1997.
[29] J.R. Tesmer, M. Nastasi, J.C. Barbour, C.J. Maggiore, J.W. Mayer, Handbook of Modern Ion Beam Materials Analysis, Materials Research Society, Pittsburgh, PA, USA, 1995.
[30] J.P. Schiffer, T.W. Bonner, R.H. Davis, F.W. Prosser Jr., Phys. Rev. 104 (1956) 1064.
[31] V.Kh. Alimov, Phys. Scr. T 108 (2004) 46.
[32] J. Crank, Mathematics of Diffusion, University Press, Oxford, 1956.
[33] T.S. Elleman, C. Alexander, R. Causey, D. Chandra, J. Fowler, A. Payne, C. Ravanbakht, L. Zumwalt, K. Verghese, Tritium transport in nonmetallic solids, in: Proceedings of Meeting on CTC Electrical Insulatory, Los Alamos, NM, CONF-76 0558, 1976, p. 163.
[34] T.S. Elleman, L.R. Zumwalt, K. Verghese, in: Proceedings of the 3rd Top. Meeting on Tech. Controlled Nuclear Fusion, Santa Fe, NM, CONF-78 0508, vol. 2, 1978, p. 763.
[35] T.S. Elleman, D. Rao, K. Verghese, L. Zumwalt, Hydrogen Diffusion, Dissolution and Permeation in Nonmetallic Solids, Report ORO-4721, 1979.
[36] K. Schnarr, H. Münzel, J. Nucl. Mater. 170 (1990) 253.
[37] K. Schnarr, H. Münzel, J. Chem. Soc. Faraday Trans. 86 (1990) 651.
[38] A. Suhaimi, R. Wölfle, S.M. Quaim, G. Stöcklin, Radiochim. Acta 40 (1986) 113.